

Experiments on Liquid Metal Flow Induced by Rotating Magnetic Dipole Moment

A. Bojarevičs, T. Beinerts

Abstract

The flow of liquid metal induced by a rotation of a cylindrical permanent magnet, which is magnetized normal to the axis, has been investigated during model experiments. Rotation of the magnetic cylinder induces a rotating magnetic field in surrounding space and consequently the vortical electrical current in conducting media. Flow in a rectangular pool of liquid metal was investigated, measuring the characteristic flow velocity as a function of angular velocity of the magnetic cylinder and distance from the axis of the magnet. Order of magnitude analysis of the induced electromagnetic force in the liquid metal pool shows that both pressure gradient and vorticity is produced, generating a complex melt motion. Combining two cylinders in a coupled rotating system allowed to achieve completely different flow patterns. Coupling of the cylinders was achieved by magnetic forces or by mechanical coupling. The variety of achievable flow patterns and magnitudes of the flow was video recorded. Suggestions are proposed to apply this type of permanent magnet systems as melt stirrers or pumps in practical tasks.

Introduction

Permanent magnet rotors are very successfully used for pumping and stirring of liquid metals [1]. Usually multipolar designs are used with permanent magnets configured as shown on the left hand schematic on Fig. 1. Considering the optimization task regarding the most

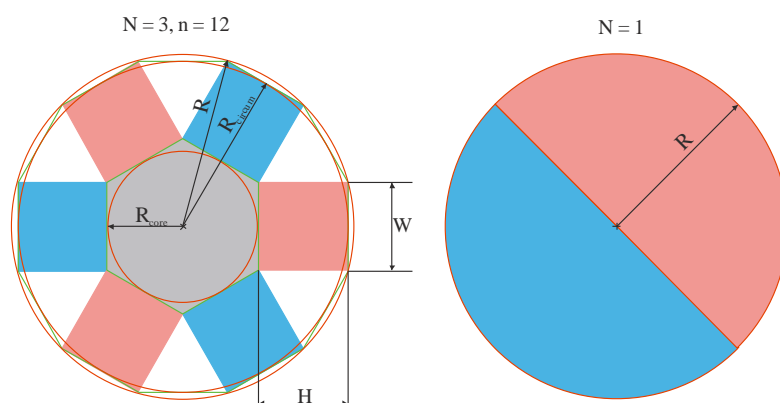


Fig. 1. Magnetic rotor with arbitrary number of magnetic pole pairs N (left) and a single magnetic dipole cylinder (right)

efficient stirring and/or pumping efficiency it was proposed that, if the distance of the liquid metal region from the surface of the magnetic rotor is not very small, a single cylindrical permanent magnet may turn out the best option [2]. Rotating magnetic cylinder produces alternating magnetic flux in the surrounding space and induces vortical electrical field. Induced current in conducting media, interacting with the magnetic field, results in electromagnetic force proportional to a square of magnetic field induction and first order of the frequency. It is obvious that a single cylindrical permanent magnet, a magnetic dipole, would produce

maximum of induction comparing to any other rotor with higher number of magnetic poles. Therefore a small scale model was built to test experimentally the feasibility of such a stirrer for practical tasks of metallurgy.

1. Description of a Cylindrical Permanent Magnet Dipole and Experimental Setup

Modern rare-earth permanent magnets tend to ideal when magnetization is nearly uniform all over the volume and relative magnetic permeability is nearing 1. Therefore, two dimensional magnetic field of a cylindrical magnet with remanence B_r , transverse to the axis of a cylinder, and radial extent $R \gg W$ (W - axial length of the magnet) at a distance L from the axis of the magnet may be given by a simple expressions in polar coordinates

$$B_r = \frac{B_r}{2} \cdot \left(\frac{R}{L}\right)^2 \cos(\omega t); B_\phi = \frac{B_r}{2} \left(\frac{R}{L}\right)^2 \sin(\omega t). \quad (1)$$

At any point in space surrounding a rotating cylindrical permanent magnet the absolute value of induction is constant but the direction of the field rotates with the same frequency ω as the cylinder rotation:

$$B = |\mathbf{B}| = \frac{B_r}{2} \left(\frac{R}{L}\right)^2. \quad (2)$$

Numerical simulation and actual measurements on the cylindrical Nd-Fe-B magnets with $R = 0.02$ m, $W = 0.08$ m and $B_r = 1.40$ T confirm that in a relevant for our experiment range of distances L , the magnetic field of a finite length W cylindrical magnet to be

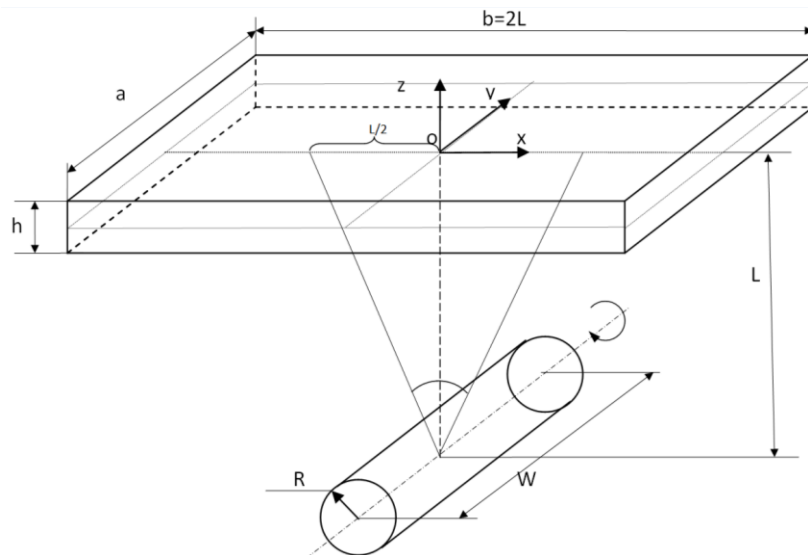
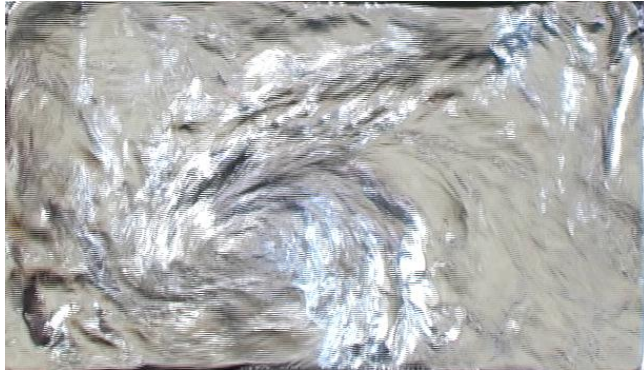


Fig. 2. A schematic of experimental setup

reasonably well described by Eq. 1 at the centre of the axial position.

Liquid metal is contained in a rectangular pool with width $a = 0.3$ m and length $b = 0.6$ m, depth of liquid metal layer is $h = 0.03$ m. The cylindrical magnetic dipole was set at distances in a range $L = (0.015 \dots 0.15)$ m beneath the melt pool. Liquid eutectic melt In-Ga-Sn were used.

Electrical conductivity of this melt at room temperature is $\sigma = 3.3 \cdot 10^6$ S/m and density $\rho = 6400$ kg/m³, speed of sound $V_s = 2740$ m/s. During tests the magnet cylinder revolved in the range of angular frequency $\omega = (6 \dots 150)$ rad/s. Higher revolutions were not achievable due to very strong unstable free surface deformation during tests, which led to multitude of gas bubbles to be entrapped into the melt. Typical picture of the free surface deformations during tests are shown on Fig. 3.



During experimental tests the characteristic velocity was measured by ultrasound Doppler anemometer inserting the probe directly into the liquid metal. Due to very pronounced large scale instability of the flow the error margin of registered time-averaged velocity was very high, up to 25%.

Fig. 3. Snapshot of the melt free surface at $L = 0.05$ m and $\omega = 80$ rad/s.

2. Experimental Test Results

Results of the measurements of time-averaged melt velocity are shown in Fig. 4. and should be considered with estimated error margin at least 25%. The mean flow pattern was extremely sensitive to very small variations of geometry regarding the alignment of axes of pool and cylindrical magnet dipole. The characteristic time of large scale pattern changes in the flow reached several minutes. So, obviously, we did not spent sufficient time to get correct average values, since melt loses to oxidation were not sponsored.

Most surprising were the mean velocity saturation at rather low frequencies at small

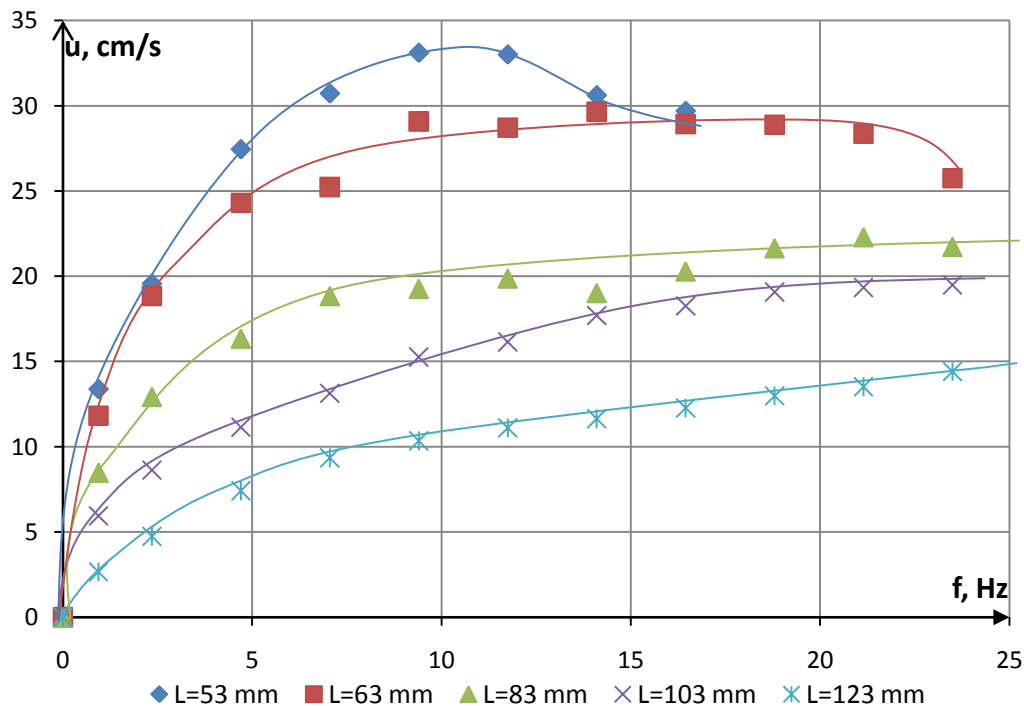


Fig. 4. Experimentally measured time-averaged velocity scale as a function of magnet dipole revolutions at five values of the distance of melt to the axis of the cylinder L

distances L of the rotor axis to the melt center. Since induced magnetic field could not be responsible for this behaviour at low frequencies, it could be suggested that increase in turbulence intensity and/or strong perturbation to liquid layer depth due to free surface deformation were the possible causes.

3. Order of Magnitude Estimates of Flow Induced by Rotating Cylindrical Dipole

For order of magnitude estimates we consider geometry similar to experimental setup schematically shown on Fig. 2. For simplicity we neglect any variation along width of the melt pool $\frac{\partial}{\partial y} \equiv 0$, except while accounting for induced current return path.

It should be noted that in order of magnitude estimates we just consider the ability of the cylindrical magnet rotor to produce translational motion, but do not account for intense vortical force created in liquid metal just above the axis of the magnet rotor. To underline it, the Fig. 4. shows results of a quasi-two-dimensional numeric simulation regarding the induced electromagnetic force distribution in the liquid metal.

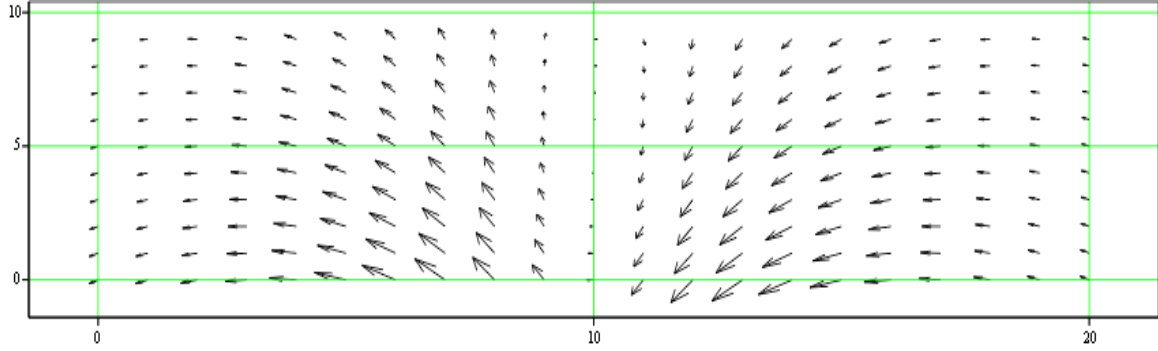


Fig. 5. Time-averaged distribution of electromagnetic force in the melt from quasi two-dimensional numeric simulation. Intense vortical component of the force is shown above the axis of the rotor

For order of magnitude estimate of the ability of cylindrical dipole to create a translational motion in a planar layer of a liquid metal following set of equations are used:

$$\left\{ \begin{array}{l} \frac{\partial(\vec{B} - \vec{B}_i)}{\partial t} = \nabla \times \vec{E} \\ \vec{j} = \sigma (\vec{E} + \vec{U} \times (\vec{B} - \vec{B}_i)) \\ \mu_0 \vec{j} = \nabla \times \vec{B}_i \\ \nabla \cdot \vec{B}_i = 0 \end{array} \right. \quad (3)$$

Choosing the characteristic amplitude value of the magnitude for the vertical component of magnetic field B_z from Eq. 2 and introducing length scales of variation in x directions equal to $L/2$ and in z direction - h , we derive a following set of order of magnitude equations:

$$\left\{ \begin{array}{l} (B - B_i) \cdot \omega = \frac{E}{L} \\ j = \sigma \cdot [E + U(B - B_i)] \\ \mu_0 j = \frac{B_{iz}}{L} - \frac{B_{ix}}{h} \\ \frac{B_{ix}}{L} + \frac{B_{iz}}{h} = 0 \end{array} \right. \quad (4)$$

Also we introduce a factor accounting for induced current return path k and aspect ratio A :

$$\begin{cases} k = \frac{1}{1 + \frac{L}{W}} \\ A = \frac{h \cdot L}{h^2 + L^2} \end{cases} \quad (5)$$

Solving the system of equations (2), (4) and (5) assuming balance between electromagnetic force and inertia force we derive following magnitude for velocity U , as a function of angular velocity of the magnetic dipole ω and distance to the melt center L .

$$U(\omega, L) = \frac{1}{\sqrt{2}} U_A(L) \frac{1}{Ind(\omega, L)} \sqrt{\frac{Ind(\omega, L)}{A(L)}}, \quad (6)$$

where

$$\begin{aligned} \Omega_d(\omega, L) &= \mu_0 \cdot \sigma \cdot \omega \cdot L \cdot h && \text{- dimensionless frequency,} \\ Sl(\omega, L) &= 1 - \frac{U}{\omega \cdot L} && \text{- slip velocity,} \\ Ind(\omega, L) &= k(L) \cdot \Omega_d(\omega, L) \cdot A(L) \cdot Sl(\omega, L) && \text{- induced field criterion,} \\ U_A(L) &= \frac{B(L)}{\sqrt{\mu_0 \cdot \rho}} && \text{- Alfven velocity.} \end{aligned}$$

Since solution for transitional velocity is a function of dimensionless criterion Ind , which in turn is a function of slip velocity Sl , which is a function of the flow velocity U , the numeric solution was found iterating by parameter U . Basic result is shown on Fig. 6.

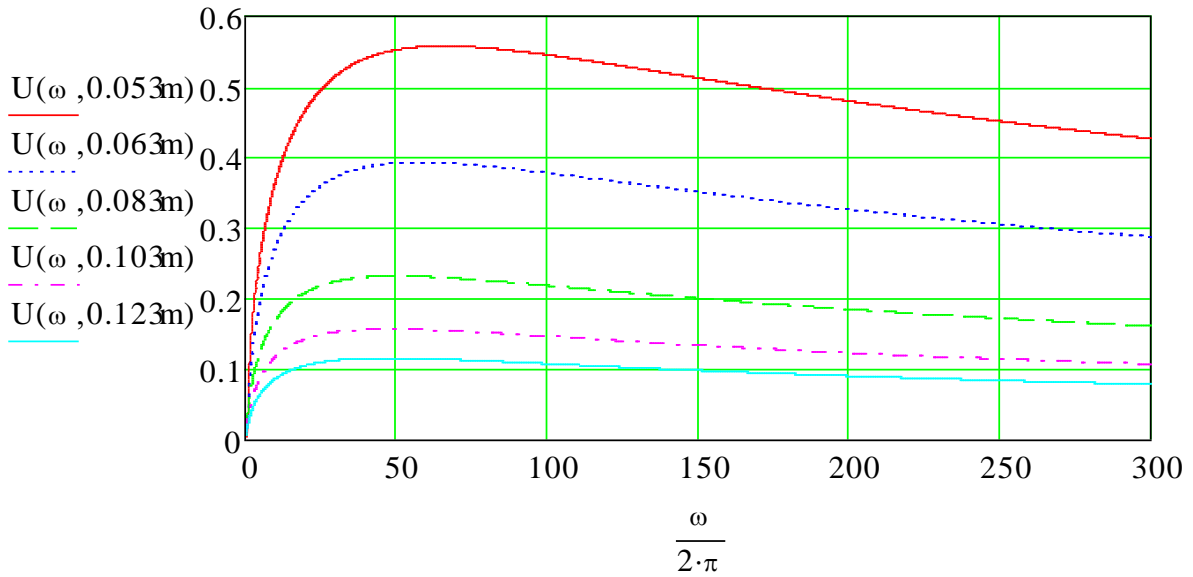


Fig. 6. Order of magnitude velocity $U(\omega, L)$ as a function of a magnetic dipole revolution frequency at five values of distance L of the cylinder axis to melt center

As it should be expected, with increase of frequency the velocity magnitude reaches a maximum and then reduces. It is obvious that induced magnetic field at high dimensionless frequencies reduces the efficiency of the magnetic cylinder dipole efficiency.

As it may be expected order of magnitude estimates deviate from the experiment quite significantly, even up to 40%. But nevertheless we consider the estimates as a first step to predict the trends at larger length scales. Moreover, since three dimensional numeric simulations, delivering a multitude of curves like given by Fig. 6. would require quite considerable computing time.

Saturation and even reduction of characteristic velocity measured during experimental tests may be argued to happen due to three dimensional flow dynamics. As already stressed we did not consider in the order of magnitude estimates the vortical part of the electromagnetic force illustrated on Fig. 5. Moreover, we did not consider the alternating magnetic flux in direction „y“ and its impact on the flow.

Assuming validity of our order of magnitude estimates, it is possible to suggest, that, for example, for liquid Aluminum contained by a wall 7 cm thick a cylindrical rotor with diameter 10 cm would be able to stir the melt with velocity up to 1 m/s.

Conclusions

After first experimental tests it seems that a cylindrical magnetic dipole rotor may be a promising option to consider for practical tasks in metallurgy for stirring or even transporting molten metal, moreover when high temperature and/or erosive action of the melt require thick refractory wall thickness of the melt containing enclosure.

References

- [1] Buceniaks I.: *Perspectives of increasing efficiency and productivity of electromagnetic induction pumps*. 14th international conference on nuclear engineering, Miami, Florida, USA, July 17-20, 2006.
- [2] Bojarevics A., Buceniaks I., Gelfgat Yu.: *Flow at the Liquid Metal Surface Subject to Rotating Magnetic Field*. PAMIR 2008, pp. 273-275.

Authors

Bojarevics, Andris
Beinerts, Toms
Institute of Physics
University of Latvia
Miera 32
LV-2159 Salaspils, Latvia
E-mail: andrisb@sal.lv
E-mail: toms.beinerts@gmail.com